Separation Science and Technology
Publication details, including instructions for authors and subscription information:
http://www.informaworld.com/smpp/title~content=t713708471

Lithium Isotope Fractionations on Inorganic Ion-Exchangers with Different Ion-Sieve Properties

Kenta Ooi[a]; Qi Feng[a]; Hirofumi Kanoh[a]; Takahiro Hirotsu[a]; Takao Oi[b]
[a] SHIKOKU NATIONAL INDUSTRIAL RESEARCH INSTITUTE, TAKAMATSU, JAPAN [b] SOPHIA UNIVERSITY, TOKYO, JAPAN

To cite this Article Ooi, Kenta , Feng, Qi , Kanoh, Hirofumi , Hirotsu, Takahiro and Oi, Takao(1995) 'Lithium Isotope Fractionations on Inorganic Ion-Exchangers with Different Ion-Sieve Properties', Separation Science and Technology, 30: 20, 3761 — 3770

To link to this Article: DOI: 10.1080/01496399508015141

URL: http://dx.doi.org/10.1080/01496399508015141

SEPARATION SCIENCE AND TECHNOLOGY, 30(20), pp. 3761–3770, 1995

Lithium Isotope Fractionations on Inorganic Ion-Exchangers with Different Ion-Sieve Properties

KENTA OOI,* QI FENG, HIROFUMI KANOH,
and TAKAHIRO HIROTSU
SHIKOKU NATIONAL INDUSTRIAL RESEARCH INSTITUTE
2217-14 HAYASHI-CHO, TAKAMATSU 761-03, JAPAN

TAKAO OI
SOPHIA UNIVERSITY
7-1 KIOICHO, CHIYODAKU, TOKYO 102, JAPAN

ABSTRACT

Lithium isotope fractionation properties were studied on five kinds of inorganic ion exchangers with different ion-sieve properties. The lithium isotope separation factors were determined batchwise in a LiOH or (LiCl + LiOH) solution at 25 or 20°C, respectively. The separation factor increased in the order birnessite-type manganese oxide < hollandite-type manganese oxide < spinel-type manganese oxides < cubic antimonic acid in the LiOH solution. It was dependent on the pore radius (r_{is}) of the ion-sieve and was a maximum at $r_{is} = 0.10$ nm. The difference in the separation factor with r_{is} could be well explained by considering two factors; the difference in hydration circumstances of Li^+ between the ion-exchanger and the solution phase, and the influence of Li^+ stabilization in the solid phase.

INTRODUCTION

Because of its low nuclear cross section for thermal neturons, ^7Li is useful for the control of corrosion and the pH of coolant waters in nuclear reactors. Lithium isotope fractionation by two-phase chemical exchange has been extensively studied in systems with a lithium amalgam (1, 2), lithium metal (3), an ion-exchange resin (4–8), and a macrocyclic polyether

---

* To whom correspondence should be addressed. Telephone: 81-878-69-3527. FAX: 81-878-69-3550.

(9, 10). However, there have been only a small number of studies (11–15) on lithium isotope fractionation with inorganic ion-exchangers since the first pioneer work by Tayler and Urey (11) with aluminosilicate. Recently, we studied the lithium isotope fractionation on spinel-type manganese oxides which have a specific selectivity for Li^+ in the aqueous phase (14). They show a significant fractionation effect with separation factors up to 1.014 at 25°C. The high fractionation effect can be explained by the difference in hydration circumstances of Li^+ between the solid and solution phases (14, 15).

Inorganic ion-exchangers have attracted attention owing to their remarkably high selectivity for certain metal ions or groups of ions (16). The specific characteristics of inorganic ion-exchangers arises partly from their rigid structure, which undergoes little swelling or shrinking in the aqueous phase. This brings about a strong steric effect or an ion-sieve effect for various ions, depending on the hydrated or dehydrated size of the adsorbing ions.

The present paper describes the lithium isotope fractionation properties of five kinds of inorganic ion-exchangers. We used spinel-type manganese oxides (redox and ion-exchange types), cubic antimonic acid, hollandite-type manganese oxide, and birnessite-type manganese oxide. The fractionation properties of these samples are discussed in terms of the pore radius of the ion-sieve.

Spinel-type manganese oxide (17) has a three-dimensional network of [1 × 3] tunnels of MnO_6 octahedra with a high selectivity for lithium ions (selectivity sequence: $Na < K < Rb < Cs \ll Li$) (18). We prepared two kinds of spinel-type samples, one showing a redox-type insertion of Li^+ and the other an ion-exchange-type insertion (19). Cubic antimonic acid has a pyrochlore structure with a high selectivity for sodium ions (selectivity sequence: $Li < K < Cs < Rb \ll Na$) (20, 21). Hollandite-type or cryptomerane-type manganese oxide has a [2 × 2] tunnel (22) which is suitable to fix metal ions (K, Rb) with an ionic size about 0.14 nm (23). The selectivity sequence is $Li < Na < Cs \ll K, Rb$. Birnessite-type manganese oxide has a layered structure (22) with an interlayer distance around 0.7 nm. It shows a high selectivity for cesium ions (selectivity sequence: $Li < K < Rb < Cs$) (24).

EXPERIMENTAL

Materials

Spinel-type manganese oxide (SpiMO-R) of the redox type was obtained by the extraction of Li^+ from $LiMn_2O_4$ spinel with acid and that of the ion-exchange type (SpiMO-I) from $Li_{1.33}Mn_{1.67}O_4$ spinel (19). The

$LiMn_2O_4$ and $Li_{1.33}Mn_{1.67}O_4$ precursors were obtained by heating mixtures of $MnCO_3$ and Li_2CO_3 with corresponding Li/Mn ratios at 800 and 400°C, respectively. The Li/Mn mole ratios of SpiMO-R and SpiMO-I were less than 0.04. Hollandite-type manganese oxide (HolMO) was obtained by passing ozone gas through $MnSO_4$ solution (with 8 M H_2SO_4) at 80°C (25). Birnessite-type manganese oxide (BirMO) was obtained by heating a mixture of Na_2CO_3 and MnOOH (Na/Mn mole ratio = 0.4) at 800°C, followed by acid treatment with 0.2 M HCl (26). The Na/Mn mole ratio of BirMo was 0.06. Cubic antimonic acid (CSbA) was purchased from TOA Chemicals Co. and used without further purification.

X-ray diffraction analyses of these materials were carried out conventionally.

Isotope Exchange

The isotope exchange study was carried out batchwise using a solution of 0.1 M LiOH or (0.03 M LiCl + 0.07 M LiOH). After mixing an ion-exchanger with the solution for 7 days, the lithium concentration in the solution was determined by atomic absorption spectrometry. The lithium ion-exchange capacity was calculated from the decrease of the lithium concentration in the solution phase relative to the initial concentration.

The $^7Li/^6Li$ isotopic ratio of the solution phase was determined by a surface ionization technique on a VG 336 mass spectrometer with a wide flight tube. The lithium species was converted to LiI by passing the solution through an anion-exchange resin followed by the addition of HI solution. A 1-μL droplet (containing 1 μg Li) was loaded onto the side filament of Re-Ta-Re triple-filament source and was dried at 70°C. The filament was loaded into the source of the mass spectrometer and subjected to isotopic analysis. Once the instrument was focused on the ^7Li peak and the Li^+-beam current was controlled to 4×10^{-11} A, the data were collected with a double collector system. The analysis was repeated four times for each sample. The internal precision was less than 0.005% on the $^7Li/^6Li$ ratio and the external precision was less than 0.2%. The isotopic separation factor (S) is defined as,

$$S = (^7\mathrm{Li}/^6\mathrm{Li})_{\mathrm{solution}}/(^7\mathrm{Li}/^6\mathrm{Li})_{\mathrm{adsorbent}} \quad (1)$$

It was calculated from the mean values of the $^7Li/^6Li$ ratio in the solution phase using the following equation:

$$S = [A(1 + A)C_0 - A(1 + A_0)C]/[A_0(1 + A)C_0 - A(1 + A_0)C] \quad (2)$$

where C_0 is the lithium concentration of the initial solution, C is that of the solution after isotopic equilibrium, A_0 is the $^7Li/^6Li$ ratio of the initial solution, and A is that of the solution after equilibration.

RESULTS AND DISCUSSION

X-Ray Analysis

X-ray diffraction patterns of the inorganic ion-exchangers are given in Fig. 1. SpiMO-R and SpiMO-I show diffraction patterns corresponding to a spinel structure, both with the lattice constant $a_0 = 0.805$ nm. HolMO gives a pattern corresponding to the hollandite structure with lattice constants $a_0 = 0.982$ nm and $c_0 = 0.285$ nm. BirMO has a birnessite structure with a d value of 0.727 nm, and CSbA has a pyrochlore structure with a lattice constant $a_0 = 1.039$ nm.

Separation Factor for Lithium Isotope

The Li^+ ion-exchange capacities of the exchangers were in the region between 3 and 5 mmol/g in the LiOH system (Table 1). Isotopic fractionations with S values above 1 are observed with these inorganic ion-exchangers, as is shown in Table 1. The S values above 1 indicate that the lighter

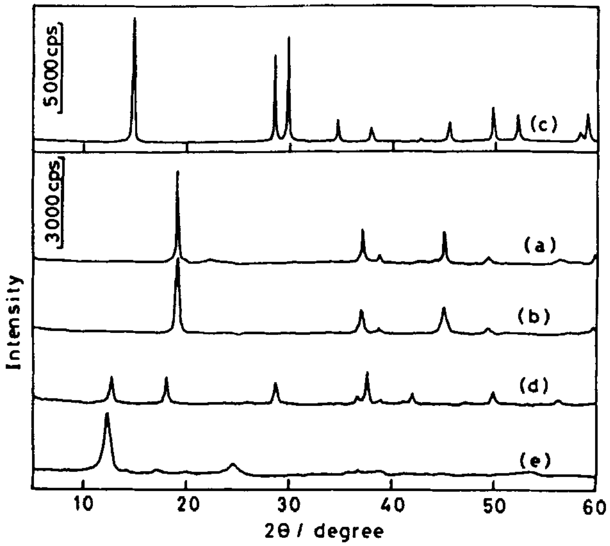

FIG. 1 X-ray diffraction patterns of inorganic ion exchangers. (a) SpiMO-R, (b) SpiMO-I, (c) CSbA, (d) HolMO, (e) BirMO.

TABLE 1
Lithium Isotope Fractionations on Inorganic Ion Exchangers

	0.1 M LiOH[a]		0.03 M LiCl + 0.07 M LiOH[b,c]	
Sample	Lithium uptake (mmol/g)	S^d	Lithium uptake (mmol/g)	S^d
SpiMO-R	3.44	1.013	1.07	1.002
SpiMO-I	5.64	1.006	1.10	0.997
CSbA	5.47	1.024	4.27	1.024
HolMO	3.73	1.006	0.85	1.006
BirMO	3.66	1.004	1.06	1.006

[a] Sample 0.10 g, solution 8 cm^3, 25°C.
[b] Sample 0.55 g, solution 8 cm^3, 20°C (SpiMO, HolMO, BirMO).
[c] Sample 0.30 g, solution 20 m^3, 20°C (CSbA).
[d] S: Separation factor, $S = (^7\text{Li}/^6\text{Li})_{\text{solution}}/(^7\text{Li}/^6\text{Li})_{\text{adsorbent}}$.

isotope ^{6}Li is fractionated in the solid phase while the heavier isotope ^{7}Li is preferentially enriched in the solution phase. The separation factor increases in the order BirMO < HolMO, SpiMO-I < SpiMO-R < CSbA. The S value for SpiMO-R agrees well with those observed in our previous study (14). The S values for SpiMO-R and CSbA are significantly larger than that (1.002) for a commercially available organic cation-exchange resin (5). It is interesting that ion-exchangers with a high selectivity for Na^+, but not for Li^+, show the highest separation factor for lithium isotope.

The Li^+ ion-exchange capacities in the (LiCl + LiOH) system are smaller (around 1 mmol/g) than those in the LiOH system, except for CSbA (Table 1). Since manganese oxides are weakly acidic ion-exchangers, they cannot adsorb Li^+ from a LiCl solution, while the acidity of CSbA is strong enough to adsorb Li^+ even from a LiCl solution. In the case of SpiMOs, the decrease of the lithium content causes a significant decrease of isotope fractionation. Our previous study (27) on ion-exchange equilibrium in the (SpiMO + LiOH) system showed that the equilibrium constant for Li^+ adsorption on SpiMO-R decreases with an increase in the lithium content, owing to the steric effects among the adsorbed Li^+. This suggests that the steric interaction among the Li^+ causes the S value to increase. Since lithium ions are in a dehydrated state in SpiMO-R, the steric interaction among Li^+ in SpiMO may be stronger than those in the other ion-exchangers. The S values of the other samples did not show such a large dependence on lithium content.

Dependence on Ion-Sieve Radius

The isotope fractionation properties are influenced by the chemical and physical structures of the ion-exchange site. We think pore structure is an important factor in the case of an ion-sieve-type adsorbent. Not only does pore size control the hydration number of Li^+ in the solid phase, but it influences the selectivity of metal ions as well. Unfortunately, the pore sizes of the present ion-exchangers are too small to determine by the conventional N_2-gas adsorption method. Thus, we introduce the pore radius (r_{is}) of an ion-sieve instead of the pore size by N_2 adsorption; r_{is} corresponds to the radius of the ion to which the ion-exchanger under consideration shows the highest selectivity. From this definition, the r_{is} values for SpiMO, CSbA, HolMO, and BirMO can be regarded as equal to the ionic radii of Li^+, Na^+, K^+, and Cs^+, respectively.

The logarithm of the separation factor is plotted against r_{is} in Fig. 2, where the ionic radii used are those calculated by Shannon and Prewitt (28). The S value shows a tendency to increase with a decrease of r_{is} up to 0.10 nm, and decreases steeply at $r_{is} < 0.10$ nm. It has been considered that the lithium isotope fractionation effects in aqueous ion-exchange systems originate mostly from the difference in hydration circumstances of Li^+ between the ion-exchanger and the solution phase (4). Since the hydration number of Li^+ in an ion-exchanger decreases with a decrease of r_{is}, we can predict that the S value increase with a decrease of r_{is}; hence SpiMO, not CSbA, should have the highest S value. The samples with $r_{is} > 0.10$ nm follow this prediction, but SpiMO does not. This suggests that

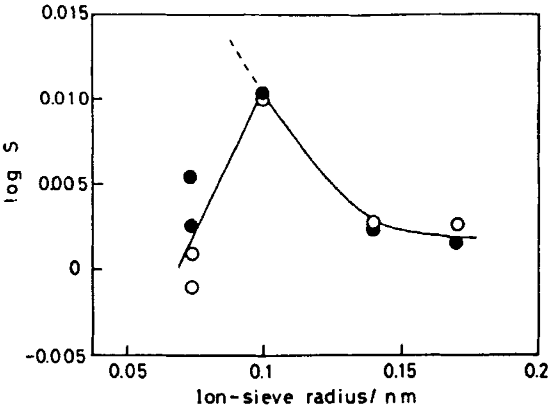

FIG. 2 Plot of log S vs ion-sieve radius. ●: LiOH system; ○: (LiOH + LiCl) system.

there is another factor that influences the lithium isotope fractionation on SpiMO, in addition to the effect of dehydration.

Model of Li^+ Isotope-Exchange Reaction

The smaller S value on SpiMOs can be explained by the effect of isotope fractionation due to Li^+ stabilization in the solid phase. The lithium isotope exchange reaction can be schematically written as in Fig. 3, where we assume hydrated Li^+ and LiOH are lithium species in the solution phase. The separation factor can then be written as

$$\ln S = \ln Kz - \ln(1 + \Delta c) \tag{3}$$

where Kz is the isotope-exchange constant for the transfer of hydrated Li^+ from the solution to the solid phase, and Δc is the isotope effect for the chemical reaction. The $\ln(1 + \Delta c)$ can be written as

$$\ln(1 + \Delta c) = \ln\{[^6\mathrm{Li(aq)}][^7\mathrm{LiOH}]/[^7\mathrm{Li(aq)}][^6\mathrm{LiOH}]\} \tag{4}$$

where Li(aq) is lithium ions in a hydrated form. The $\ln(1 + \Delta c)$ value is constant when the solution phase has the same chemical composition. The $\ln Kz$ can be written as in Eq. (5) by considering an imaginary cycle (Fig. 3):

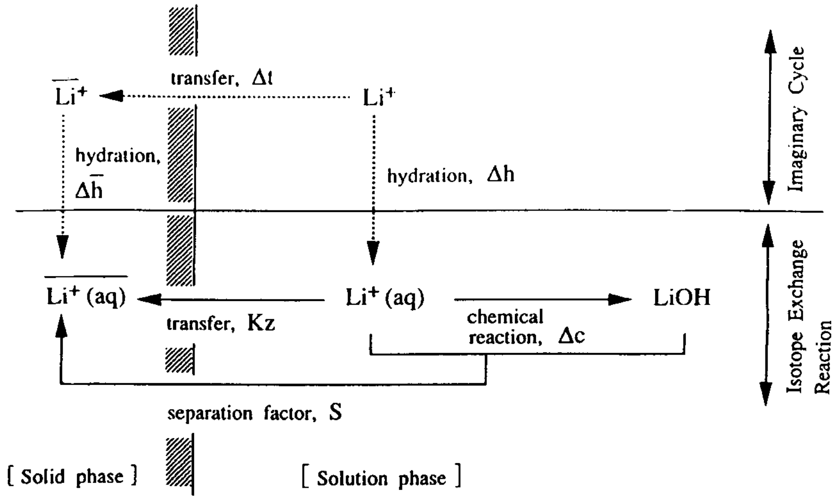

FIG. 3 Schematic diagram for lithium isotope fractionation reaction.

$$\begin{aligned}\ln Kz &= \ln\{[^7\mathrm{Li(aq)}][^6\overline{\mathrm{Li(aq)}}]/[^7\overline{\mathrm{Li(aq)}}][^6\mathrm{Li(aq)}]\}\\ &= \ln\{[^7\mathrm{Li}][^6\overline{\mathrm{Li}}]/[^7\overline{\mathrm{Li}}][^6\mathrm{Li}]\} - \ln\{[^7\mathrm{Li}][^6\mathrm{Li(aq)}]/[^7\mathrm{Li(aq)}][^6\mathrm{Li}]\}\\ &\quad + \ln\{[^7\overline{\mathrm{Li}}][^6\overline{\mathrm{Li(aq)}}]/[^7\overline{\mathrm{Li(aq)}}][^6\overline{\mathrm{Li}}]\}\\ &= \ln(1 + \Delta t) - \ln(1 + \Delta h) + \ln(1 + \Delta \bar{h}) \qquad (5)\end{aligned}$$

where an overbar represents a chemical species in the solid phase. Δt is the isotope effect for the transfer of dehydrated Li^+ to the solid phase, and Δh and $\Delta \bar{h}$ are those for the hydration of Li^+ in the solution phase and the solid phase, respectively. The sum of the second and third terms on the right-hand side corresponds to the isotope effect owing to the difference in hydration circumstances of Li^+ between the solid and solution phases. The $\ln(1 + \Delta h)$ has a negative constant value in the aqueous phase. The $\ln(1 + \Delta \bar{h})$ value is equal to $\ln(1 + \Delta h)$ when Li^+ are in a fully hydrated form in the solid phase; it approaches zero with a decrease of the hydration number. Therefore, the isotope effect by the difference in hydration circumstances, $-\ln(1 + \Delta h) + \ln(1 + \Delta \bar{h})$, increases with a decrease of r_{is} owing to the decrease of hydration number of Li^+ in the solid phase. The r_{is} dependence of $\ln S$ in the region above 0.10 nm can be well explained by the difference in hydration circumstances.

Effect of Li$^+$ Stabilization

The smaller S value on SpiMOs can be explained by considering the $\ln(1 + \Delta t)$ term. The $\ln(1 + \Delta t)$ value varies depending on the state of Li^+ ions (in dehydrated form) in the solid phase. They are surrounded by the oxygen atoms which form the pore surfaces of the metal oxide system. The electrostatic and steric interactions between Li^+ and the oxygen atoms may bring about an isotope fractionation effect similar to that on hydration. We think that these interactions are correlated with the Li^+ selectivity of an ion-exchange reaction. The stronger the attractive interaction, the higher the Li^+ selectivity may be.

Since SpiMO has a strong affinity to Li^+, the Li^+ in SpiMO are tightly fixed at the tetrahedral sites of the cubic closed-packed oxygen framework of the spinel structure. They are surrounded by the adjacent four oxygens in a tetragonal arrangement. Since this Li—O arrangement is close to that of hydrated Li^+, the isotope effect $[\ln(1 + \Delta t)]$ for the transfer may resemble that $[\ln(1 + \Delta h)]$ for Li^+ hydration in the solution phase. Therefore, we can conclude from Eq. (5) that Li^+ stabilization in the solid phase compensates in large part for the isotope effect due to the dehydration of Li^+ in the solid phase. The small S value on SPiMOs may arise from the effect of isotope fractionation due to Li^+ stabilization in the solid phase.

Inorganic ion-exchangers other than SpiMOs show low selectivity for Li^+, suggesting a low interaction between Li^+ and the oxygen atoms. The $\ln(1 + \Delta t)$ values may be much smaller on these samples than those on SpiMOs. CSbA shows low selectivity for Li^+ but has a relatively small r_{is} value. Therefore, isotope fractionation by the dehydration of Li^+ may not be compensated for by the effect due to Li^+ stabilization in the solid phase. The present result suggests that the ion-exchanger with small r_{is} as well as low affinity for Li^+ has a high fractionation effect for lithium isotope. The large separation factor (9) which has been observed in the (Li^+ + 2,2,1-cryptand) system supports this idea, since 2,2,1-cryptand shows the highest affinity to Na^+ among alkali metal ions.

The above results imply that we can obtain an adsorbent with a high fractionation effect to lithium isotope by searching for ion-exchangers with an ion-sieve radius around 0.1 nm (or with the Na^+ ion-sieve property).

REFERENCES

1. A. A. Palko, J. S. Drury, and G. M. Begun, *J. Chem. Phys.*, *64*, 1828 (1976).
2. K. Okuyama, I. Okada, and N. Saito, *J. Inorg. Nucl. Chem.*, *35*, 2883 (1973).
3. G. Singh, J. C. Hall, and P. A. Rock, *J. Chem. Phys.*, *56*, 1855 (1972). G. Singh and P. A. Rock, *Ibid.*, *57*, 5556 (1972). J. C. Hall, L. F. Silvester, G. Singh, and P. A. Rock, *Ibid.*, *59*, 6358 (1973).
4. D. A. Lee and G. M. Begun, *J. Am. Chem. Soc.*, *81*, 2332 (1959). D. A. Lee, *J. Phys. Chem.*, *64*, 187 (1960).
5. Z. Hagiwara and Y. Takakura, *J. Nucl. Sci. Technol.*, *6*, 279, 326 (1969).
6. A. R. Gupta, *Sep. Sci. Technol.*, *14*, 843 (1979).
7. S. Fujine, *Ibid.*, *17*, 1049 (1982).
8. T. Oi, A. Kondo, E. Ohno, and M. Hosoe, *Z. Naturforsch.*, *48a*, 811 (1993).
9. K. Nishizawa, H. Watanabe, S. Ishino, and M. Shinagawa, *J. Nucl. Sci. Technol.*, *21*, 133 (1984). K. Nishizawa and H. Watanabe, *Ibid.*, *23*, 843 (1986). K. Nishizawa, T. Takano, I. Ikeda, and M. Okahara, *Sep. Sci. Technol.*, *23*, 333 (1988).
10. S. Fujine, K. Saito, and K. Shiba, *J. Nucl. Sci. Technol.*, *20*, 439 (1983).
11. T. I. Tayler and H. C. Urey, *J. Chem. Phys.*, *5*, 597 (1937).
12. E. Glueckauf, K. H. Barker, and G. P. Kitt, *Disc. Faraday Soc.*, *7*, 199 (1949).
13. H. Kakihana and M. Aida, *Bull. Tokyo Inst. Technol.*, *116*, 39 (1973).
14. T. Oi, H. Ogino, N. Izawa, H. Kakihana, K. Ooi, Y. Miyai, and S. Katoh, *Proc. Int. Conf. Ion Exch., ICIE'91*, Tokyo, October 2–4, 1991, p. 613.
15. T. Oi and A. Takeguchi, *Bull. Soc. Sea Water Sci.*, *47*, 69 (1993) (in Japanese).
16. A. Clearfield (Ed.), *Inorganic Ion Exchange Materials*, CRC Press, Boca Raton, Florida, 1982.
17. J. C. Hunter, *J. Solid State Chem.*, *39*, 142 (1981).
18. K. Ooi, Y. Miyai, and S. Katoh, *Solv. Extr. Ion Exch.*, *5*, 561 (1987).
19. Q. Feng, Y. Miyai, H. Kanoh, and K. Ooi, *Langmuir*, *8*, 1861 (1992).
20. M. Abe, *J. Inorg. Nucl. Chem.*, *41*, 85 (1979).
21. M. Abe, *Bull. Chem. Soc. Jpn.*, *42*, 2683 (1969).
22. R. G. Burns and V. M. Burns, in *Manganese Dioxide Symposium, Vol. 2, Tokyo, 1980*

(B. Schumm Jr., H. M. Joseph, and A. Kozawa, Eds.), I.C. MnO_2 Sample Office, Cleveland, Ohio, 1981, p. 97.

23. M. Tsuji and M. Abe, *Solv. Extr. Ion Exch.*, *2*, 253 (1984).
24. K. Ooi, Doctoral Thesis, Tokyo Institute of Technology, 1991.
25. T. Nishimura and Y. Umetsu, *Shigen Sozai Gakkaishi*, *108*, 373 (1992).
26. S. Hirano, R. Narita, and S. Naka, *Mater. Res. Bull.*, *19*, 1229 (1984).
27. K. Ooi, Y. Miyai, S. Katoh, H. Maeda, and M. Abe, *Langmuir*, *6*, 289 (1990).
28. R. D. Shannon and C. T. Prewitt, *Acta Crystallogr.*, *B52*, 925 (1969).

Received by editor December 19, 1994